Progress In Electromagnetics Research B, Vol. 11, 205–222, 2009

AN ULTRA WIDEBAND IMPULSE OPTOELECTRONIC RADAR: RUGBI

M. Lalande, J. C. Diot, S. Vauchamp, and J. Andrieu

XLIM/IUT GEII
7 rue Jules Vallès, 19100 Brive, France

V. Bertrand

CISTEME, ESTER
BP 6913, 87069, Limoges Cedex, France

B. Beillard, B. Vergne, V. Couderc, and A. Barthélémy

XLIM/Université de Limoges
123 Av. A. Thomas, 87060 Limoges Cedex, France

D. Gontier

Commissariat à l'Energie Atomique
BP n°12, 91680 Bruyères-le-Châtel, France

R. Guillerey

DGA/CELAR
BP 7419, 35174 Bruz Cedex, France

M. Brishoual

DGA/SPART
7 rue des Mathurins, 92 211 Bagneux Cedex, France

Abstract—An ultra wideband radar system based on a coherent emission of an ultra-wideband antenna array using photoconductive switching devices is proposed. The triggering process is obtained by the excitation of semiconductor samples in linear mode using a picosecond laser source. The emitting antenna system and the receiving antenna developed by the Research Institute XLIM present some specific qualities suitable for radiation and measurement of ultra-short pulses. The optical control of the sources allows to sum the

radiated power and to steer the transient radiation beam accurately. The experiments realized with this optoelectronic array validate these two concepts. Another way of improving these systems is proposed. It involves using bipolar pulse generators.

1. INTRODUCTION

Since 1996, XLIM Institute has developed some Ultra Wideband (UWB) systems applied to Radar Cross Section (RCS) measurement [1] or UWB Synthetic Aperture Radar (SAR) like PULSAR for mines detection [2]. PULSAR system has shown difficulties to realize antennas which have a wide bandwidth [300 MHz–3 GHz] and can support high voltage (maximum peak level supply: 25 kV obtained in 2002). These difficulties limit the UWB radar capabilities in particularly range, resolution and dynamic sensitivity of UWB impulse radars.

To extend limits of impulse UWB radar, a solution consists of UWB antennas array utilization. On the other hand, high-power UWB pulse radiation source with a peak power higher than 10^{10} W is necessary for solving a number of tasks. Realization of this type of source is possible on the basis of multi element arrays [3, 4].

To achieve higher field level, XLIM has chosen a radiation system including n generators/n antennas instead of a single source which is not easy to build and to match the antenna. The objective is to drive UWB antenna array since the rise time and the shape of the radiated pulse is influenced by the jitters of the sources. So this jitter must be as small as possible.

In this paper, such a system in which four photoconductive switches generating high voltage pulses supply four UWB antennas is presented.

The UWB antennas designed especially for this transient UWB radar system are able to radiate high power pulses with a minimum of distortion. Indeed, the radiated or the received pulse are not very spread. The generation of high voltage ultra-short pulses with low jitter is obtained by optically activated photoconductive semiconductor switches in the linear mode [5–7]. This photoconductive generation technique allows to feed an UWB antenna array with a perfect time synchronization.

UWB transient radars are fed by monopolar signals generally (Gaussian or biexponential shapes). In this case, low frequency coupling signals between transmit and receive antennas limit the dynamic sensitivity. In this paper, the excitation of the emitting

antenna by a monocycle signal (bipolar pulse) is envisaged to increase the signal to clutter ratio.

2. EXPERIMENTAL SETUP

The experimental setup is shown in Fig. 1.

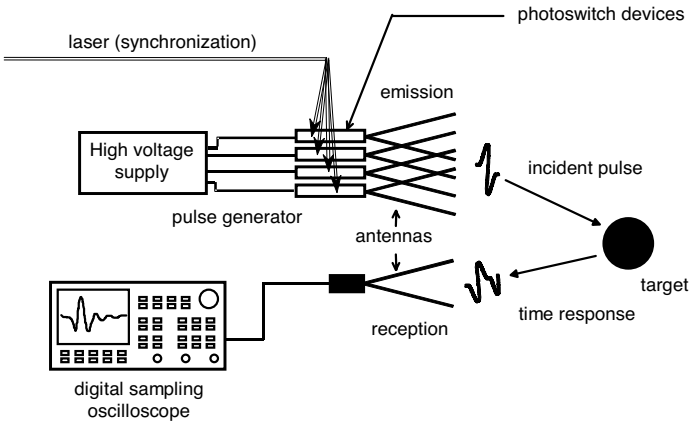

Figure 1. Impulse optoelectronic UWB antenna array in radar configuration.

It consists in four UWB photoconductive generators producing 300 ps pulses with 10 kV of peak voltage. These generators are synchronized using a single picosecond Nd:YAG laser source delivering pulses of 25 ps at 1064 nm. A large part of the spectrum contained in the switched electrical pulses is simultaneously radiated by four identical UWB antennas. Each of them can support an input voltage level up to 10 kV. The signal diffracted by the target is detected with another UWB antenna [8] connected to a real time oscilloscope. Its sampling rate is 20 Gs/s and its analog bandwidth is 7 GHz.

2.1. A. Optoelectronic Pulse Generator

2.1.1. Bi-exponential Generator

The optoelectronic generator [9] is composed of a photoconductive semiconductor coupled with a capacitor (Fig. 2). This capacitor is charged by using a continuous high voltage supply. The photoexcitation of the switch increases the conductivity of the semiconductor. Consequently, a rapid discharge causes the

propagation of an electrical pulse in the 50 Ω output line. The duration and shape of the transient current depend significantly on the optical excitation, the carrier life time, the bandwidth of the generator components and the stored electrical energy.

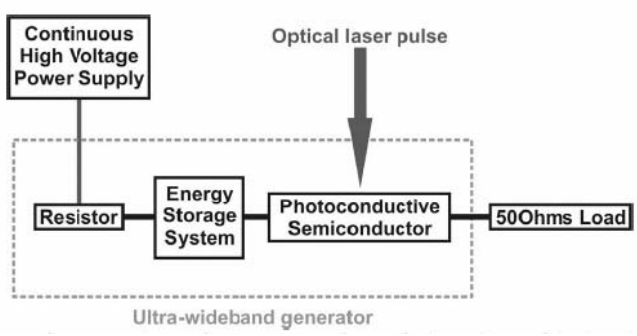

Figure 2. Schematic representation of the optoelectronic pulse generator.

Using the innovative technology of the French Atomic Energy Commission (CEA), we achieved the following high power performances by polarizing the under test generator (Fig. 3) with a voltage level of 16 kV: FWHM of 300 ps, rise time of 130 ps and peak level of 10.7 kV by using optical energy of 1.2 mJ. From our knowledge, this value is the lowest currently obtained in the linear mode.

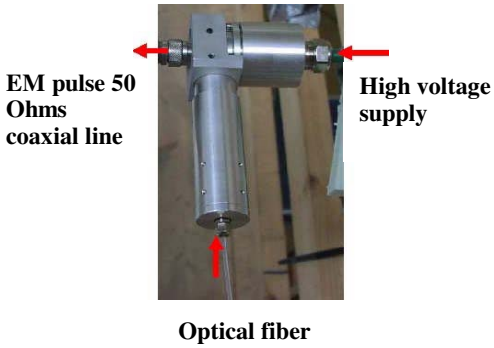

Figure 3. Optoelectronic generator.

The shape and the normalized spectrum of the electrical pulses are shown in Fig. 4. Note that this component has an unlimited life time because it works in linear mode.

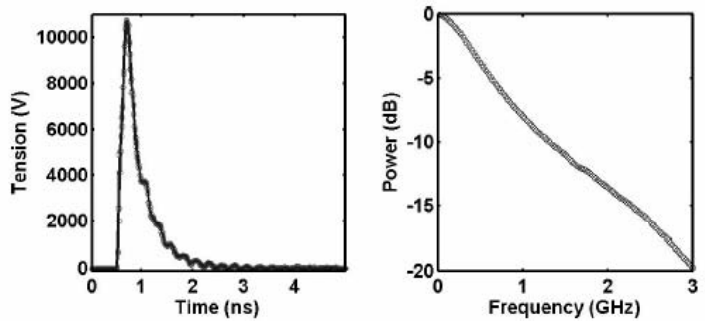

Figure 4. Example of biexponential pulse and normalized spectrum obtained with optoelectronic generator: peak level.

2.1.2. Monocycle Generator

These photoconductive switches are also suitable for the generation of bipolar pulses [10] by using the principle of the frozen wave generator. It consists in a section of transmission line with 50 Ω impedance and two photoconductive switches. At the input, a photoconductive switch P1 shunts the transmission line while at the output end the line is connected to the matched impedance via a second switch P2. During the off state, the storage line is fully charged and open-circuit at both ends (Fig. 5(a)). When both switches are closed simultaneously, we can simplify the working order with the following sequence. The forward wave V+ delivers a positive voltage to the load. The backward wave V− is reflected from the short-circuit end, and undergoes an inversion. Thus, a pulse of negative polarity is delivered to the load, immediately following the positive pulse (Fig. 5(b)). The bipolar pulse duration depends directly on the charged line length.

We realize a generator of bipolar pulses by using two similar semiconductors. The bias voltage used to polarize the two switches is fixed at 5 kV. Under these conditions, we obtain a bipolar pulse with a peak to peak voltage of 3 kV which represents a switching efficiency of 60%. The two photoconductive semiconductors are optically triggered with a total optical energy lower than 1 mJ.

The profile and the spectrum content of the electrical pulses can be modified by using time delay between the two switches. A square pulse, an unbalanced and a balanced bipolar pulse are obtained and shown in Fig. 6. The content of the generated frequency spectrum is then largely affected and exhibits low amount of low frequency for a synchronous activation of the two switches. The perfect control of the delay between the two input optical pulses can be directly linked to the spectral content of the pulse spectrum.

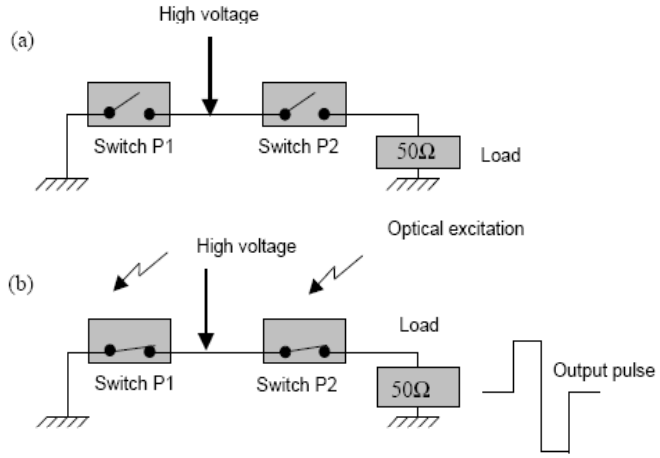

Figure 5. Principle of the bipolar pulse generator.

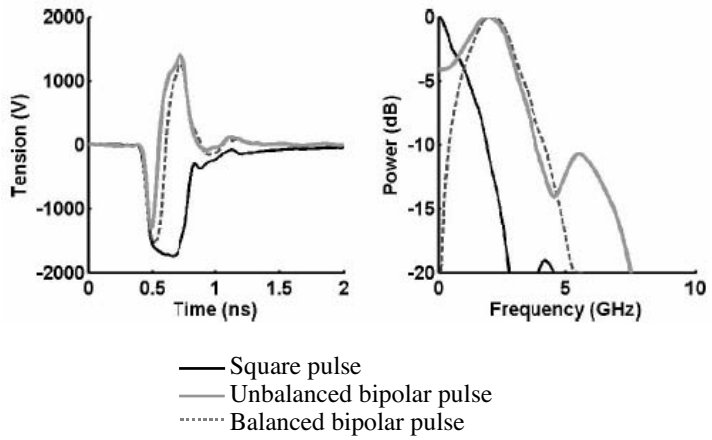

Figure 6. Waveform and spectrum of different bipolar pulses with peak to peak level of 3 kV and total duration of 450 ps.

2.1.3. Optical Control System of Generators

The optical control system of generators is presented in Fig. 7. The beam emitted by the Nd:YAG laser is aligned in the table by a periscope. Four identical laser beams are created by using a set of beam splitters and mirrors. Then these four beams are put orward by optical delay lines and injected into optical fibres that trigger off the

four generators. Delay lines allow to set the delay between the different laser pulses. The pulse triggering is perfectly controlled. The precision of synchronization (including jitter) is lower than 5 ps.

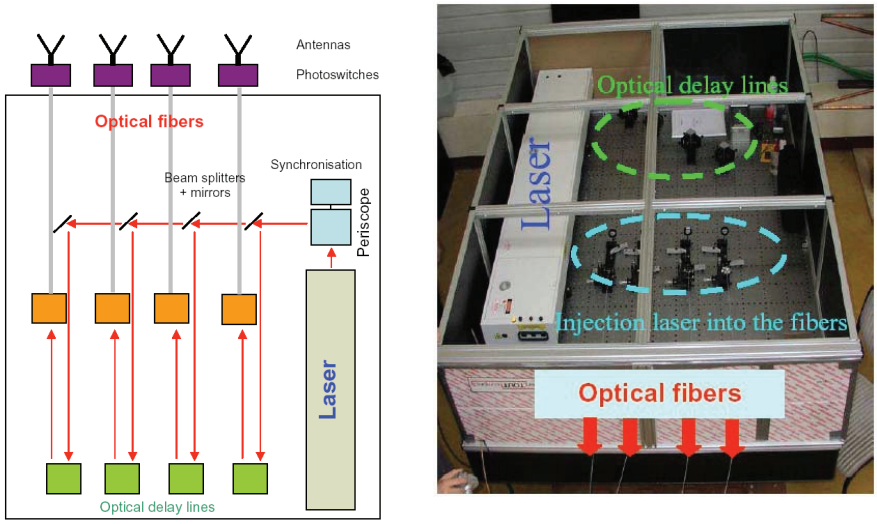

Figure 7. Optical control system of generators.

2.2. Emitting UWB Antennas: Valentine Antennas

The Valentine antenna [11] is a traveling wave antenna. It is able to radiate high power pulses with a minimum of distortion: the radiated or the received pulse should not be distorted or spread. It is made up of a copper strip curved along a specific profile. The width of the metallic strip is 52 mm and the other dimensions of the antenna are given in Fig. 8. The input of the antenna is a symmetrical two strips transmission line with Teflon between the two strips in order to limit the risk of electrical breakdown. A 50 Ω input impedance is fixed by appropriate dimensions of the input line. After the section of the transmission line, the strips flare according to an exponential profile and return according to a circular form.

A balun is required between the generator and the antenna. The balun is a mechanical transition between the 50 Ω coaxial output of the generator and the 50 Ω double-strip input of the antenna. Moreover, it permits to feed the antenna with a symmetrical mode. It eliminates the even mode, which modifies the antenna radiation. The antenna and its associated balun were realized by Europulse Company (Lot, France).

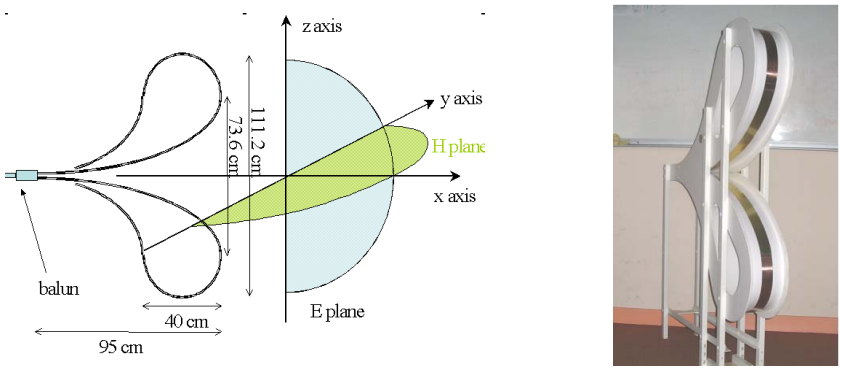

Figure 8. Dimensions of Valentine antenna.

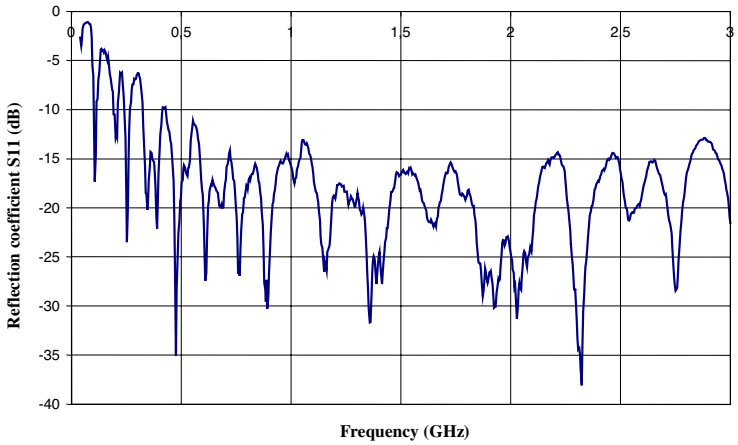

Figure 9. Reflection parameter of the Valentine antenna.

Figure 9 shows the measured reflection coefficient of the balun-antenna system. A S11 maximum level of −10 dB is obtained in the frequency range 300 MHz–3 GHz. The axial gain is deduced from a transient measurement method [8] for a frequency range of 300 MHz–3 GHz (Fig. 10). The results show a quite good agreement between the theoretical and experimental gains (The balun is not represented in the simulation). The gain is about 9 dB in the frequency range 400 MHz–1 GHz and it varies between 10 dB at 12 dB in the frequency range of 1 GHz–3 GHz.

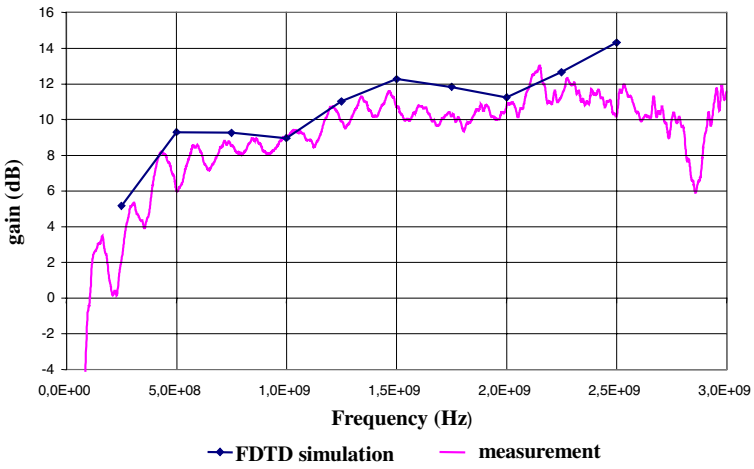

Figure 10. Gain of the Valentine antenna.

2.3. Receiving UWB Antenna: Dragonfly Antenna [8]

The receiving antenna, named "Dragonfly" antenna, was developed for a previous UWB radar system [12]. This antenna is made up of four metallic flared plates with a 50 Ω input impedance (Fig. 11). The input antenna is a symmetrical double-strip transmission line. In order to build the radiation part, each input strip is divided in two flared plates. The balun ensures the transition between a 50 Ω coaxial cable and the 50 Ω input impedance fixed by the input planar configuration.

Figure 11. Dragonfly antenna.

The main characteristics of this antenna are: a bandwidth of 250 MHz–3 GHz (−10 dB) and a gain about 12 dB in the frequency

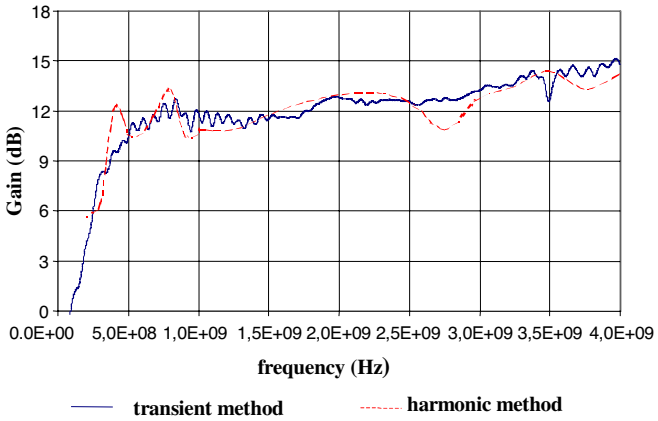

Figure 12. Gain of the Dragonfly antenna.

range from 500 MHz to 3 GHz (Fig. 12). A comparison of the dragonfly antenna gain is presented in Fig. 12 for transient [13] and harmonic measurements. We notice a good agreement between the two measurements.

3. RESULTS

3.1. Increase of Radiated Power with the Array: Improvement of the Radar Range

The array consists of four Valentine antennas 35 cm away from each others (Fig. 13). Each antenna is fed by a photoswitch generating biexponential pulses. Optical delay lines are adjusted to synchronise the different excitation pulses. The radiated field is measured at 8 m along the array axis by a Dragonfly UWB antenna (250 MHz–3 GHz) connected to the real time digital oscilloscope [11].

Fig. 14 presents the measured transient waveforms respectively for one, two, three or four transmitting antennas. For this analysis, all the antennas keep their position in the array. For the case where two antennas are fed, comparison of radiation of the pair of antennas at the central position or at the extremities of the array has been done. The electric field level is proportional to the antenna number. The transient shapes are identical and dispersion does not appear.

Fig. 15 presents the Fourier transform of previous signals (Fig. 14). For an antenna doubling, a 6 dB·V increase is observed. The increase of power is validated on the whole frequency bandwidth. At higher frequencies, we notice a difference between the cases where the two supplied antennas are close and the cases where they are far away.

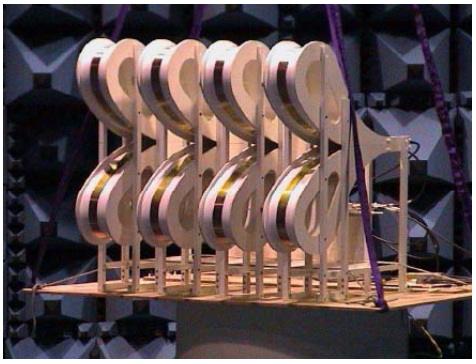

Figure 13. Array of four Valentine antennas.

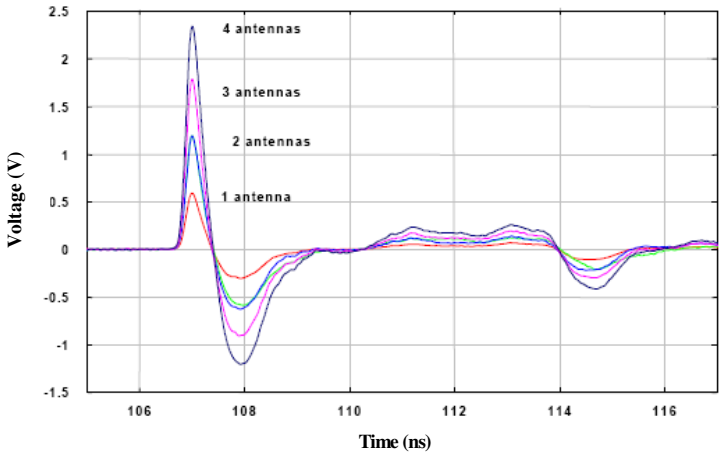

Figure 14. Received signals generated by the array of four Valentine antennas.

3.2. Increase of Directivity and Beam Steering

The graph which represents the transient electric field as function of time and angle is a suitable UWB radiation source descriptor [14]. Fig. 16 represents this type of characteristic for three cases: a) one antenna is excited only, b) the four antennas are excited simultaneously c) the four antennas are excited with time delays corresponding to 10° steering.

Each antenna of the array is excited by 1 kV bi-exponential pulse. The system is positioned on an automatic turntable. Optical delays are adjusted to point the radiation beam along an angle of 0° (array

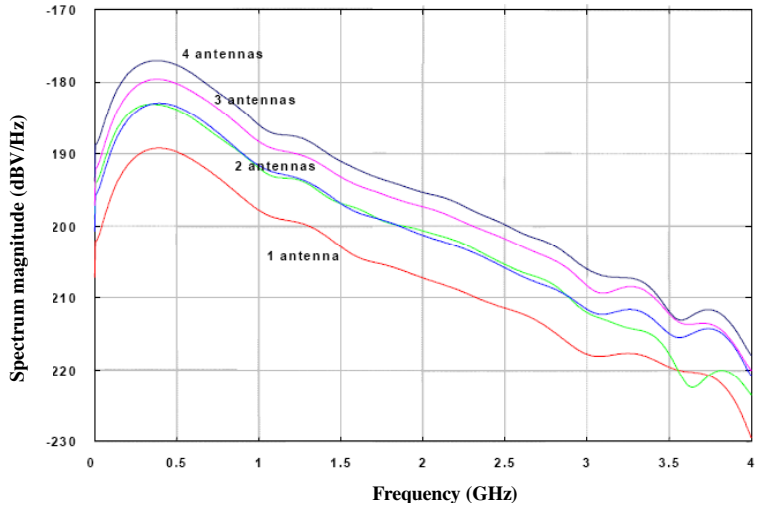

Figure 15. Fourier Transform of radiated signals.

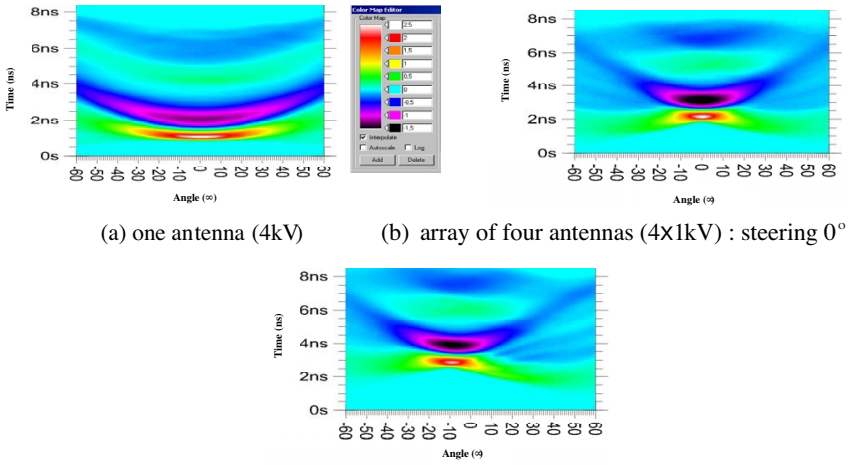

(a) one antenna (4kV) (b) array of four antennas (4X1kV) : steering 0°

(c) array of four antennas (4X1kV): steering 10°

Figure 16. Transient radiation patterns.

axis) or along an angle of 10°.

Comparisons are made with the electromagnetic behaviour of a simple antenna excited by a 4 kV driving pulse.

The graphs given in Fig. 16 allow to notice that:

- The array effect can be observed: high focusing of electromagnetic

energy.

- The beam steering is correctly realized.
- The signal shape is similar along the radiation principal axis for two steering adjustments.

So, the choice of distance between the antennas is good with a feed by bi-exponential pulses.

The possibility to drive each photoswitch with optical timedelay lines (accuracy < 5 ps) permits to point the radiation beam between $-20°$ and $+20°$.

The realization of this type of optical sources antenna array allows to increase radar range, to scan, to point and to track with electronic driving antennas.

At the same time, high power electronic generators are developed with less and less important trigger jitter. For example, available on the market, fast power generator delivering pulses with amplitude of 50 kV, rise time less than 200 ps, with a repetition frequency of 1 kHz presents a trigger jitter less than 20 ps. The integration of such a generator in a multi element system becomes possible when the highest spectral frequency of the radiation pulse is less than 2 GHz.

3.3. Advantage of a Monocycle Excitation

3.3.1. Pulse Emitted by Optoelectronic Generator

Figure 17 shows two examples of pulse emitted by the optoelectronic generator.

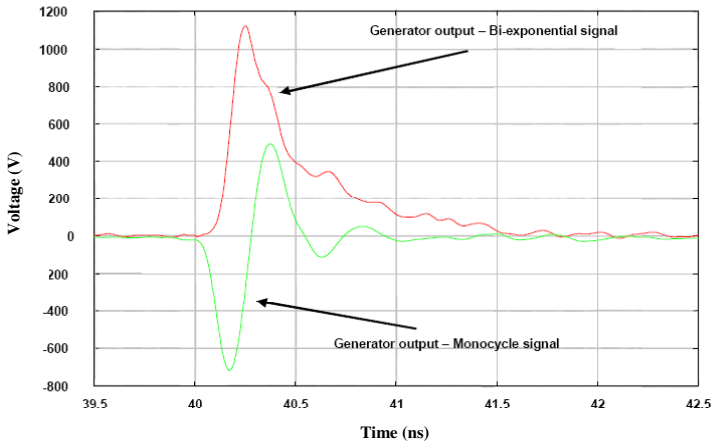

Figure 17. Generated pulses by optoelectronic devices.

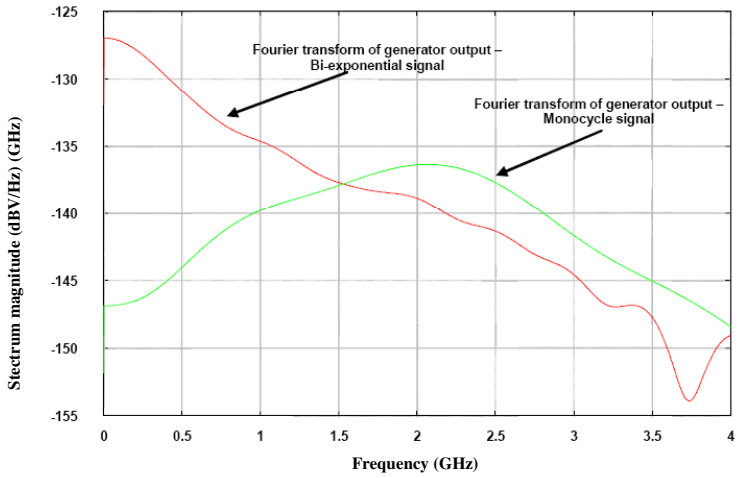

Figure 18. Fourier transform of generated pulses.

The first is bi-exponential pulse. The second is a pulse with mean value equal to zero. The rise time is 100 ps for the bi-exponential pulse and 96 ps for the monocycle pulse. Fig. 18 shows the Fourier transforms of these pulses. Energy is distributed on higher frequencies when a monocycle signal is used.

3.3.2. Pulse on the Output of Receiving Antenna

For the study of influence of exciting waveform on the receiving pulse, only one Valentine antenna is used for transmission and a Dragonfly antenna is used for the reception. The antennas are positioned facing each other at a distance of 6 m. Fig. 19 shows the pulses on the output of the receiving antenna when the transmitting antenna is supplied by the pulses reported on Fig. 17. The spread of the pulse is lower than 300 ps with the monocycle signal (1 ns with the bi-exponential signal). In addition, there are no oscillation and rebound after the main pulse with the monocycle excitation.

Figure 20 shows the Fourier transform of these pulses. A strong difference between the spectrum of bi-exponential and monocycle pulses can be observed, as expected. The maximum of energy is at low frequency (between 300 MHz and 700 MHz) for bi-exponential pulse and the energy is better distributed on the frequency band of the monocycle pulse (400 MHz–2.5 GHz).

In the next test, the receiving antenna is placed beside transmitting antenna (radar setup). Coupling signal is measured on the output of receiving antenna (Fig. 21).

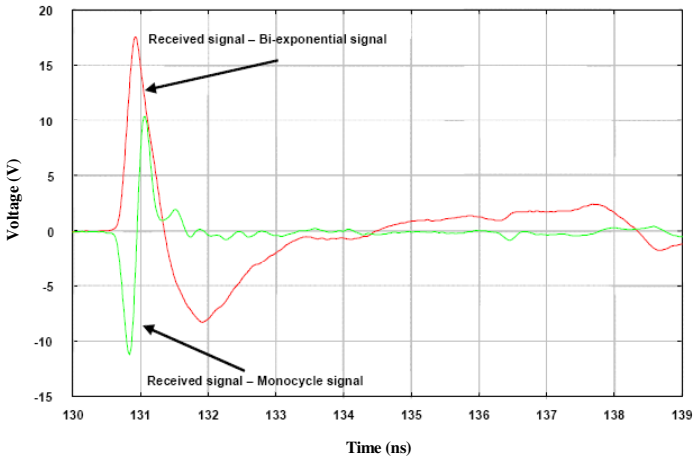

Figure 19. Received pulses for two excitation waveforms.

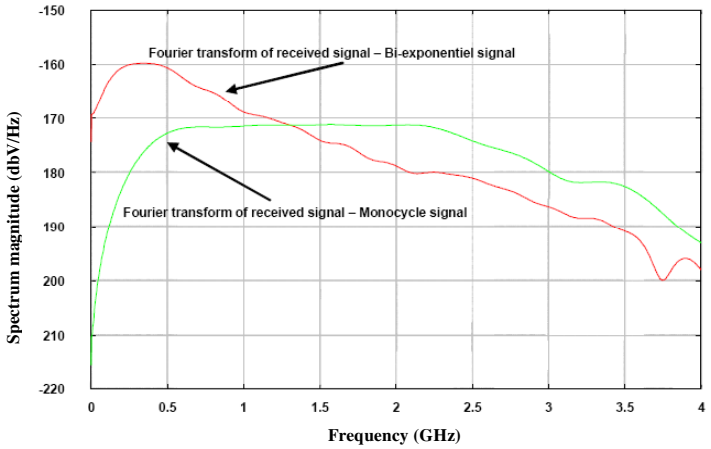

Figure 20. Spectral magnitude of the received pulses for two excitation waveforms.

This coupling level is strongly reduced with the monocycle signal. The coupling mean level is divided by 20. This advantage allows to view the future with optimism. Attenuators for protecting the digital oscilloscope and the subtraction numerical treatment in the time domain for eliminating the coupling signals and isolate target responses are not necessary. So the dynamic sensitivity of such a system will be improved.

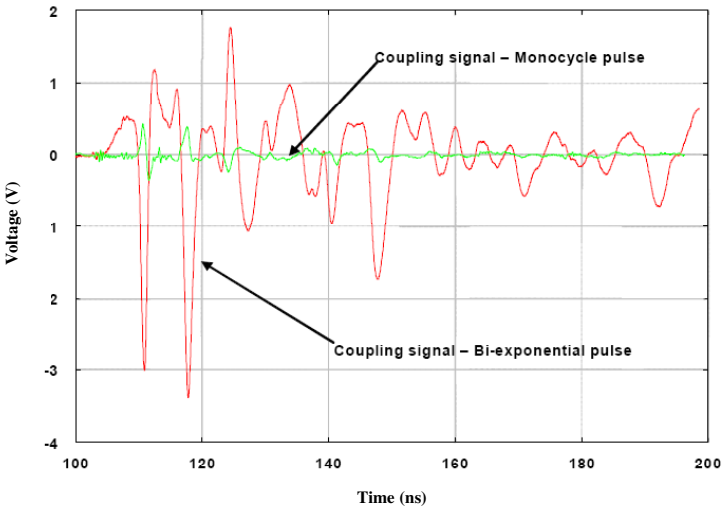

Figure 21. Coupling signals measured on the receiving antenna (radar configuration) for bi-exponential and monocycle driving pulses.

4. CONCLUSION

The current limits (range, resolution and dynamic sensitivity) of UWB impulse radars can be extended by using radiation system including n antennas/n generators. This system architecture presents the advantage that the radiation power increases with the source number. The more important difficulty in developing such system is the difficulty of limiting the jitter between radiation sources. A solution consists of impulse optoelectronic systems. Optical systems with ultrafast laser sources generate without jitter ultrashort electrical waveforms. The optical control of the sources allows to sum the radiated power and to steer the transient radiation beam accurately. The advantage of the architecture n generators/n antennas is the working continuity even if an elementary source is defective.

The possibility to program driving monocycle signals allows to optimise the system according to the application bandwidth, such as foliage, ground and wall penetrating radars. The spectrum content choice is possible by controlling the transient waveform.

In the future, it will be necessary to calculate the dimensions of the array antenna according to the excitation signal shape. A miniaturization of the antennas is being studied.

The future operational system will be capable to scan, to point and to track with electronic driving antennas, combining waveform control

with beam steering. These performances are to authorize developments in other domains such as EMC and HPM.

ACKNOWLEDGMENT

This work was supported by the French Armament Procurement Agency DGA and the Research Institute XLIM wishes to acknowledge it. The authors also would like to thank I.D.R.I.S. (Institute for Development and Resources in Intensive Scientific Computing) for their help with data processing (NEC SX-5).

REFERENCES

1. Chevalier, Y., Y. Imbs, B. Beillard, J. Andrieu, M. Jouvet, B. Jecko, M. Le Goff, and E. Legros, "UWB measurements of canonical targets and rcs determination," *EUROEM'98*, Tel Aviv-Israël, June 14–19, 1998.
2. Gallais, F., J. Andrieu, B. Beillard, Y. Imbs, V. Malpeyre, B. Jecko, and M. Le Goff, "A new ultra wide band short pulse, radar system for mine detection," *Ultra Wide Band, Short-Pulse Electromagnetics*, P. D. Smith and S. R. Cloude (eds.), Vol. 5, 175–182, Kluwer Academic/Plenium Publishers, New York, USA, 2002.
3. Koshelev, V. I., V. P. Gubanov, A. M. Efremov, S. D. Korovin, B. M. Kovalchuk, V. V. Plisko, A. S. Stepchenko, and K. N. Sukhushin, "High-power ultrawideband radiation source with multielement array antenna," *13th International Symposium in High Current Electronics*, 2004.
4. Efremov, A. M., V. I. Koshelev, B. M. Kovalchuk, V. V. Plisko, and K. N. Sukhushin, "Source of high-power ultrawideband radiation wave beams with orthogonal polarization," *14th International Symposium in High Current Electronics*, Tomks, Russia, September 2006.
5. Auston, D. H., "Picosecond optoelectronic switching and gating in silicon," *Appl. Phys. Lett.*, Vol. 26, 101–103, 1975.
6. Antonetti, A., M. M. Malley, G. Mourou, and A. Orszag, "A high power switching with picosecond precision: Applications to high speed Kerr cell and pockels cell," *Opt. Comm.*, Vol. 23, No. 3, 435, 1977.
7. Holzman, J. F., F. E. Vermeulen, and A. Y. Elezzabi, "Ultrafast photoconductive self-switching of subpicosecond electrical pulses,"

IEEE Journal of Quantum Electronics, Vol. 36, No. 2, 130–136, 2000.

8. Delmote, P., C. Dubois, J. Andrieu, V. Bertrand, M. Lalande, B. Beillard, B. Jecko, R. Guillerey, F. Monnier, M. Le Goff, L. Pecastaing, A. Gibert, J. Paillol, and P. Domens, "The UWB-SAR system PULSAR: New generator and antenna developments," *SPIE'S 17th Annual International Symposium on Aerospace/Defense Sensing, Simulation, and Controls*, Orlando, Florida, USA, April 21–23, 2003.
9. Vergne, B., V. Couderc, A. Barthelemy, M. Lalande, V. Bertrand, and D. Gontier, "High-power ultra-wideband electrical pulse generation by using doped silicon photoconductive switch," *Microwave and Optical Technology Letters*, Vol. 48, No. 1, 121–125, January 2006.
10. Vergne, B., V. Couderc, A. Barthelemy, M. Lalande, V. Bertrand, and D. Gontier, "Unipolar and bipolar electrical pulse generator using photoconductive semiconductor switches," *SPIE Symposium on Optics/Photonics in Security & Defense*, Bruges, Belgium, September 26–29, 2005.
11. Diot, J. C., P. Delmote, J. Andrieu, M. Lalande, V. Bertrand, B. Jecko, S. Colson, R. Guillerey, and M. Brishoual, "A novel ultra-wide band antenna for transient UWB applications in the frequency band 300 MHz–3 GHz: The Valentine antenna," *IEEE Antennas and Propagation*, Vol. 55, No. 3, 987–990, March 2007.
12. Gallais, F., J. Andrieu, B. Beillard, Y. Imbs, V. Malpeyre, B. Jecko, and M. Le Goff, "A new ultra wide band Short Pulse Radar system for mine detection," *Ultra-Wide Band, Short-Pulse Electromagnetics*, P. D. Smith and S. R. Cloude (eds.), Vol. 5, 175–182,, Kluwer Academic/Plenum Publishers, New York, USA, 2002.
13. Andrieu, J., S. Nouvet, V. Bertrand, B. Beillard, and B. Jecko, "Transient characterization of a novel ultra-wide band antenna: The scissors antenna," *IEEE Transactions on Antennas and Propagation*, Vol. 53, No. 4, 1254–1261, April 2005.
14. Salo, G. R. and J. S. Gwynne, "UWB antenna characterization and optimization methodologies," *Ultra-Wideband Short-Pulse Electromagnetics 6*, Mokole et al. (eds.), 329–336, Kluwer Academic/Plenium Publishers, 2003.